UNIVERSITY OF CALIFORNIA

SANTA CRUZ

METHYLATION OF HISTONE H3 LYSINE-9 REGULATES HEMATOPOIETIC STEM CELL DIFFERENTIATION

A thesis submitted in partial satisfaction
of the requirements for the degree of

MASTER OF ARTS

in

MOLECULAR, CELL, AND
DEVELOPMENTAL BIOLOGY

by

Rebekah M. Sousae

December 2014

The Thesis of Rebekah M. Sousae is approved:

_____
Camilla Forsberg, Ph.D., chair

_____
Manuel Ares Jr., Ph.D.

_____
Susan Strome, Ph.D.

_____
Tyrus Miller
Vice Provost and Dean of Graduate Studies

TABLE OF CONTENTS

ABSTRACT

Rebekah M. Sousae

Methylation of H3K9 regulates hematopoietic stem cell differentiation

Epigenetic mechanisms clearly play a role in determining stem cell identity, but the details of how they contribute remain undefined. Previously, our lab has shown that hematopoietic stem cell (HSC) differentiation involves a progressive, global accumulation of heterochromatin in the cell nucleus. Our goal is to characterize the mechanisms behind this process by investigating the role of the histone methyltransferase G9a, which promotes heterochromatin formation during HSC differentiation. Treatment of HSCs *in vitro* with UNC0638, a selective inhibitor of G9a, leads to an accumulation of hematopoietic progenitors. Global gene expression analysis reveals that UNC0638 treated cells have higher expression of genes involved in HSC function, including several transcription factors such as *Sox6* and *Gata1*. Overall these data indicate that heterochromatin formation, mediated in part through G9a-mediated histone methylation, is necessary for the transition of HSCs into more mature cells and identifies global chromatin condensation as an essential regulator of stem cell lineage potential and differentiation.

DEDICATION

This thesis is dedicated to the people in my life whose daily support outside the lab made this thesis possible- Nicholas Stuart Furnal, My Parents, My Family and Emily Mitchell Strait.

ACKNOWLEGDMENTS

I would like to acknowledge the following people for their expertise and involvement in this thesis project:

[1]Fernando Ugarte: Postdoctoral research scientist

[1]Gabriela Sanchez: Undergraduate research student (Mentor: Rebekah Sousae)

[3]Bertrand Cinquin: Collaborating scientist

[1]Jana Krietsch: Postdoctoral research scientist

[1, 4]Eric Martin: CIRM Bridges Trainee

Hannah Zhang: High School Research Intern (Mentor: Rebekah Sousae)

Tara Thakurta: High School Research Intern (Mentor: Rebekah Sousae)

[2] Jessica Perez- Cunningham: Graduate research student

[1,2] Camilla Forsberg: Principal Investigator and mentor

[1]Institute for the Biology of Stem Cells; Department of Biomolecular Engineering; University of California Santa Cruz; Santa Cruz, CA USA

[2]Program in Biomedical Sciences and Engineering; Department of Molecular, Cell and Developmental Biology; University of California Santa Cruz; Santa Cruz, CA USA

[3]National Center for X-ray Tomography, University of California, San Francisco and Lawrence Berkeley National Laboratory, Berkeley, CA 94720, USA

[4]CIRM Bridges Program; San Jose State University; San Jose, CA USA

FIGURE/ EXPERIMENTAL CONTRIBUTIONS

Figure 1. (A) Tree: Sousae, SXT Images: Ugarte, Cinquin, *(B-C) Ugarte, Cinquin

Figure 2. *(A-B) Sousae: assisted by Sanchez

Figure 3. (A) Sousae (B) Sousae, Ugarte (C-E) Sousae: assisted by Zhang, Thakurta *(E: HSC fold difference data)

Figure 4. (A-B) Sousae

Figure 5. (A-B) Sousae

Figure 6. *(A-E) Sousae and Ugarte, *(F) Ugarte

Figure 7. *(A) Sousae, (B-C) Transplants: Sousae; Bleeds: Sousae or Sanchez or Martin or Krietsch; Bleed data analysis: Sousae

Figure 8. (A) Sousae, *(B) Transplants: Sousae or Ugarte; Bleeds: Sousae or Ugarte or Sanchez; Bleed data analysis: Sousae or Ugarte, (C-D) Sousae

Figure 9. (A) Sousae, *(B) Transplants: Sousae or Ugarte, Bleeds: Sousae or Ugarte or Sanchez; Bleed data analysis: Sousae or Ugarte

*Experiment is included in manuscript in submission:

Fernando Ugarte, Rebekah Sousae, Bertrand Cinquin, Gabriela Sanchez, Margaux Inman, Herman Tsang, Matthew Warr, Emmanuelle Passegué, Carolyn Larabell, E. Camilla Forsberg. “Progressive chromatin condensation and H3K9 methylation regulate the differentiation of embryonic and hematopoietic stem cells.” Under Review

KEY TERMS

General Terms

BM: Bone Marrow

EM: Electron Microscopy

SXT: Soft X-ray Tomography

Nomenclature for Cell Types

ESC: Embryonic Stem Cell

HSC: Hematopoietic Stem Cell; cells capable of producing all mature hematopoietic lineages and self-renewal

MPP: Multipotent Progenitor; cells capable of producing all mature hematopoietic lineages with limited self-renewal capabilities

CMP: Common Myeloid Progenitors, a type of myeloid progenitor capable of producing MEPs and/or GMPs

MEP: Myeloid- Erythroid Progenitor

GMP: Granulocyte-Macrophage Progenitor

CLP: Common Lymphoid Progenitor

RBC: Red Blood Cell

GM: Granulocytes/ Macrophages

Nomenclature for Cell Populations

HSPC: (Includes MPPs & HSCs) Hematopoietic Stem and Progenitor Cells (also known phenotypically as KLS)

KLS: (Includes MPPs & HSCs) cells expressing the surface proteins c-kit and Sca1, but not those marking mature hematopoietic lineages [Lin] ($c\text{-}Kit^{+}/Lin^{-}/Sca1^{+}$)

MyPro: (Includes CMP, MEP, and GMP populations) Myeloid Progenitors; cells capable of producing mature myeloid lineages. Cells expressing the surface proteins c-kit, but not Sca1 or those marking mature hematopoietic lineages [Lin] ($c\text{-}Kit^{+}/Lin^{-}/Sca1^{-}$)

INTRODUCTION

In humans, mature blood cells are produced at a rate of more than 1 million cells per second (Seita et. al 2010; Ogawa, 1993). These cells originate from a rare population of multipotent hematopoietic stem cells (HSCs) that reside in the bone marrow. HSCs are mostly quiescent, but are also capable of differentiating when necessary to generate all mature blood cell types. Therefore, understanding the balance between self-renewal and differentiation is a key to unlocking the mechanisms of regulation of hematopoiesis.

While the hierarchy and lineage potential of hematopoietic cell populations is well characterized (Boyer et al., 2011; Forsberg et al., 2006), our understanding of their epigenetic control is limited by difficulties in measuring chromatin parameters in rare HSC populations or differentiation intermediates. Only recently have open chromatin regions of hematopoietic progenitor populations been explored using ATAC-seq (Buenrostro et al., 2013; Lara-Astiaso et al., 2014), a technique that requires far lower cell numbers compared to traditional methods such as DNase-seq or FAIRE-seq. Although some progress has been made in mapping chromatin modifications in HSCs and their progeny, there are major gaps in our understanding of the characteristics of chromatin structure and remodeling upon HSC differentiation.

We are only beginning to understand the functional consequences of large-scale chromatin remodeling and identify how master regulators of chromatin architecture

control hematopoietic lineage potential. For example, transcription factors such as C/EBPα have been shown to protect adult HSCs from apoptosis and promote quiescence by maintaining chromatin configurations (Hasemann et al., 2014). Importantly, epigenetic mechanisms and chromatin dynamics are misregulated in many hematopoietic diseases. Several types of leukemia are characterized by dramatic changes in H3K79 (Histone 3 Lysine 79) methylation arising from chromosomal translocations affecting the activity of the chromatin remodeling protein DOT1L (Krivtsov et al., 2008). Understanding the role of chromatin modifications during HSC differentiation will not only help us investigate mechanisms of disease, but will also aid us in understanding stem cell fate and lineage decisions.

In a first attempt to understand the role of chromatin dynamics during hematopoiesis, our lab previously characterized global chromatin changes that take place during HSC differentiation into subsequent lineages. Imaging by electron microscopy (EM) and soft x-ray tomography (SXT) allowed us to analyze the entire chromatin content of cells, quantifying the total volumes of hetero- vs. euchromatin (McDermott et al., 2009; Ugarte, Sousae et al, under review). Similar to embryonic stem cells (ESCs), HSC euchromatin content significantly decreases upon differentiation, condensing into highly packed heterochromatin (Figure 1A-C). This finding is supported by DNase I sensitivity assays which suggest similar progressive chromatin condensation from pluripotent ESCs, to HSCs, and to mature blood cells (Ugarte, Sousae et al, in

submission). From these data, it is clear that lineage potential is reflected in global chromatin composition. In order to understand the relationship between chromatin organization and stem cell differentiation, we sought to identify specific chromatin modifications that might act as regulators. By targeting key silencing marks, we hope to elucidate how heterochromatin formation affects HSC differentiation potential.

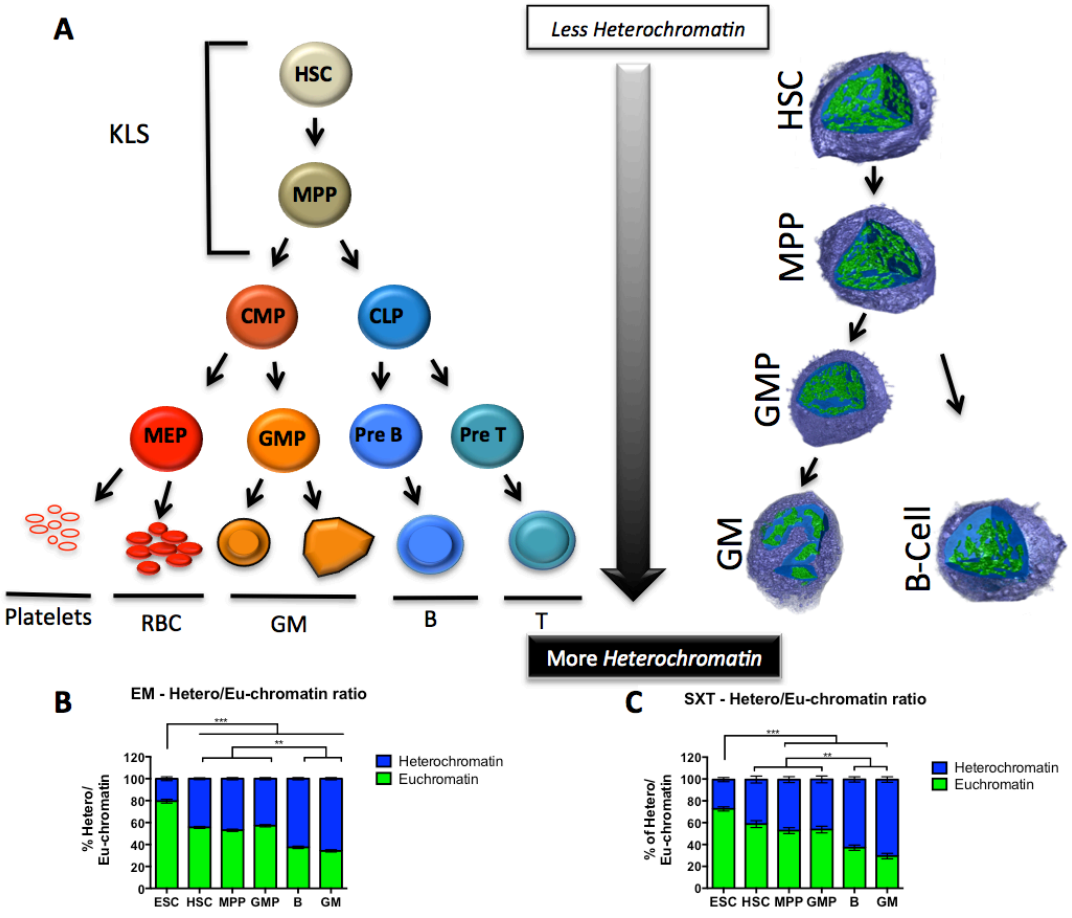

Figure 1. Chromatin condenses during hematopoietic differentiation. As HSCs differentiate, euchromatin condenses, increasing heterochromatin. (A) Hematopoietic lineage tree (left) displays HSC and MPP as multipotent KLS. Soft X-ray tomography (right) displays the organization of hetero (blue nuclear regions) and euchromatin (green nuclear regions) in a three-dimensional reconstruction *(Ugarte, Sousae et al., in submission)*. (B) Quantification of the ratios of heterochromatin and euchromatin by EM and (C) volume by SXT revealed significant reductions in the proportion of euchromatin upon stem cell differentiation (EM, n=30; SXT, n=8; per cell type).

RESULTS

G9a inhibition leads to progenitor cell accumulation *in vitro.*

To identify key molecular regulators of chromatin condensation during HSC differentiation we tested several small molecule inhibitors of chromatin modifiers in *in vitro* HSC differentiation experiments. Five chromatin modifier inhibitors were selected: UNC0638, a G9a (Ehmt2) inhibitor (Vedadi et al., 2011); Decitabine, a cytosine analog that interferes with DNA methylation (Stresemann and Lyko, 2008); EPZ-5675, an inhibitor of Dot1L, writer of H3K79me (Daigle et al., 2013); DZnep, an inhibitor of Ezh2, writer of H3K27me3 (Miranda et al., 2009); and SGI-1027, an inhibitor of Dnmt1 and Dnmt3a (Datta et al., 2009).

Each inhibitor was titrated to determine toxicity and incubated with freshly isolated HSCs grown on AFT024 fetal liver stromal feeder layer (Moore et al., 1997) for five days (Figure 2A). AFT024 provide similar signaling which mimics in vivo stem cell developmental compartments and provide an *in vitro* growth system that maintains quantitative levels of functional HSCs for longer periods of time than liquid culture (Moore et al., 1997; Wineman et al., 2006). Only inhibition of G9a led to a clear hematopoietic phenotype - a significant accumulation of hematopoietic stem and progenitor cells (HSPC), also known as KLS (c-Kit^{+}/Lin^{-}/Sca1^{+}; cells expressing the surface proteins c-kit and Sca1, but not those marking mature hematopoietic lineages [Lin]). UNC0638 inhibits G9a by blocking substrate access to the SET domain (Vedadi et al., 2011). G9a mono- and di-methylates Histone H3 lysine 9 (H3K9) in

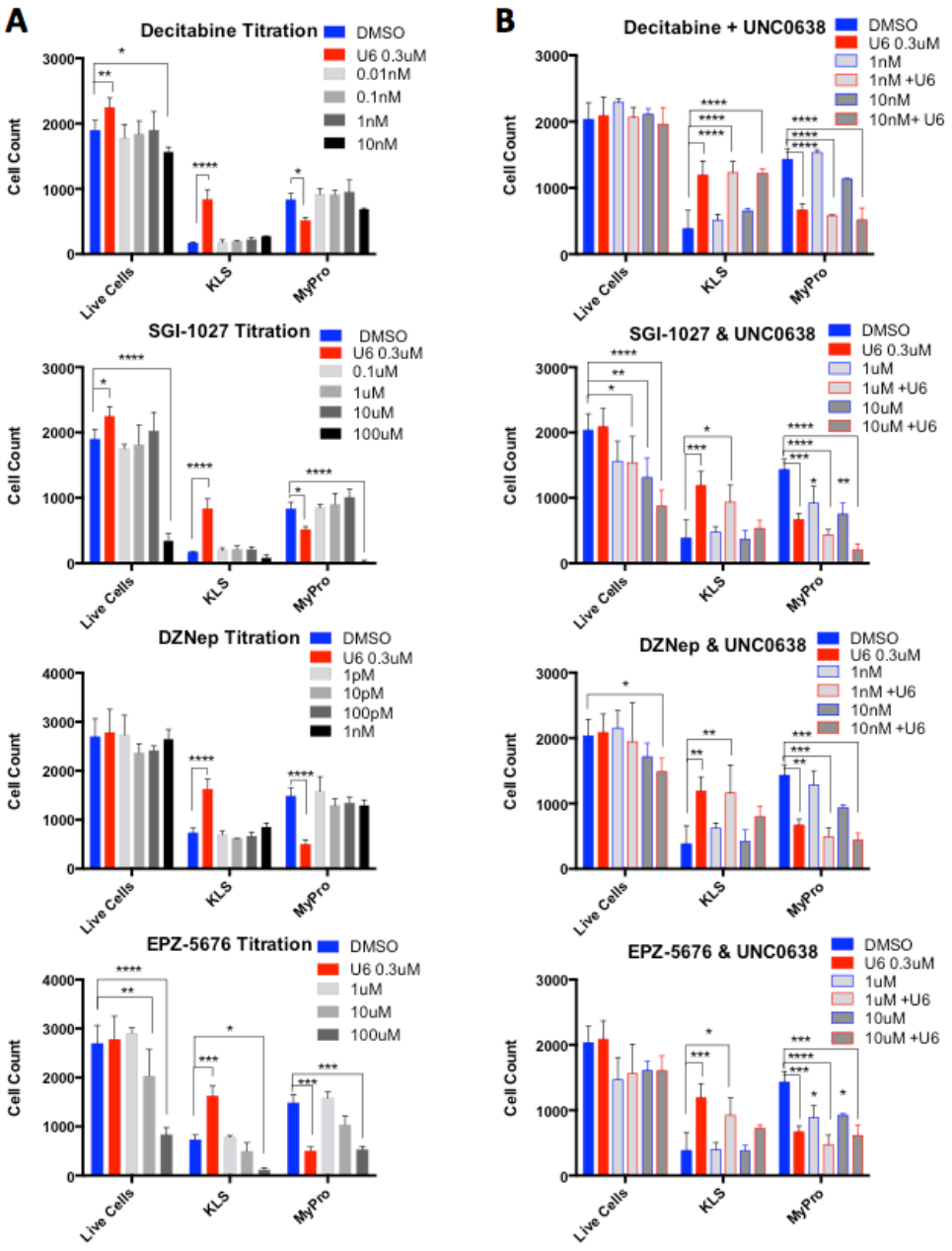

Figure 2. G9a inhibition uniquely leads to stem and progenitor cell accumulation *in vitro.* (A) Live cells, KLS fraction, and MyPro fraction after 5 days of in vitro culture of mouse HSCs on AFT-024 feeder layer with Decitabine (DNA Methylation Inhibitor), SGI-1027 (Dnmt3a/3b and Dnmt1 inhibitor), DZNep (Ezh2 inhibitor), or EPZ-5676 (DOT1L inhibitor). Incubation with UNC0638 (U6) alone lead to an increase in KLS cells at the cost of MyPro population. (B) Inhibitors cultured with 0.3uM UNC0638 still showed similar phenotype as UNC0638 treatment alone.
P-values were determined using two-way ANOVA and Dunnett's multiple comparisons p*≤ 0.05, p**≤ 0.01, p***≤ 0.001, p****≤ 0.0001

euchromatin domains and promotes heterochromatin formation (Tachibana et al., 2002; Kubicek et al., 2007). Furthermore, G9a deficient embryonic stem cells exhibit severe differentiation defects, suggesting G9a's involvement in (lineage) commitment and differentiation (Tachibana et al., 2002). The other 4 inhibitors targeting DNA methylation, H3K79me, and H3K27me3 failed to confer a hematopoietic phenotype at non-toxic concentrations, and failed to enhance effects in combination with UNC0638 (Figure 2B). Therefore, under the above conditions, only inhibition of the chromatin modifier G9a impairs HSC differentiation.

Accumulation of KLS cells upon G9a inhibition occurred both in co-culture with AFT cells and in liquid culture conditions. Titrating the UNC0638 drug on HSCs in liquid culture revealed that the concentration range used with AFT layers still produced a significant increase in KLS with no significant loss in viability up to a 1μM concentration (Figure 2, 3B). Therefore, we continued to use UNC0638 at 0.3μM (the same concentration identified in an initial screen on AFT024 feeder layers) in liquid culture for subsequent experiments.

Stem and progenitor cells require G9a for proper differentiation

One possibility is that G9a inhibition leads to an increase in stem and progenitors by promoting self-renewal. In order to address the relationship between G9a inhibition and self-renewal, we further characterized the inhibitor's effect on other cell types such as multipotent progenitors (MPPs), which have limited self-renewal capabilities

compared to HSCs. We also included common myeloid progenitors (CMPs), which have no regenerative properties and rapidly differentiate into mature hematopoietic cells during 2–3 cell divisions in primary culture (Akashi et al., 2000).

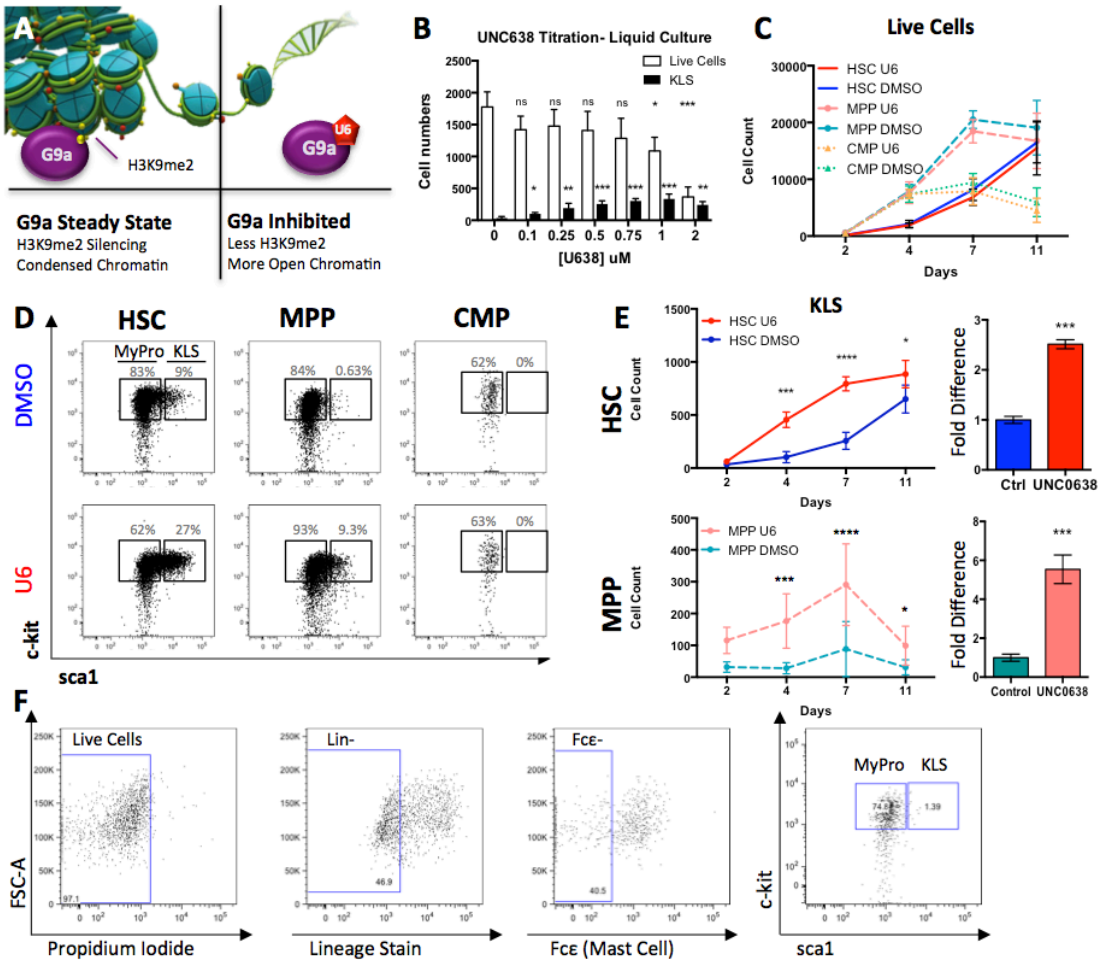

Figure 3. G9a inhibition of HSCs and MPPs leads to an accumulation of stem and progenitor population. (A) Schematic representation of G9a and its inhibitor UNC0638. (B) Numbers of live cells and KLS cells after 5 days of in vitro liquid culture of 500 mouse HSCs with the UNC0638 at varying concentrations. n=4 wells in two independent experiments. (C-E) 200 HSCs, 500 MPPs, or 500 CMPs were seeded in Xvivo15 media containing SCF, TPO, Flt-3, IL-3, GM-CSF with & without UNC0638. Total numbers of live cells (C) or KLS (D-E) were counted after five days of culture (3 wells n=3) (D) FACS plots of MyPro & KLS pregated on lin-, Fcε- fraction. (F) Gating Strategy for isolating and analyzing cultured, live, Lin-, Fcε-, MyPro or KLS. Fcε is used to gate out mast cells, which phenotypically appear c-kit^{+} & sca1^{+}. P-values were determined using two-way ANOVA p*≤ 0.05, p**≤ 0.01, p***≤ 0.001, p****≤ 0.0001

Treatment of HSCs, MPPs, and CMPs with UNC0638 had no effect on cell viability or overall cell numbers (Figure 3C). G9a inhibition lead to an accumulation of KLS cells when starting with isolated HSC and MPP populations, but not when starting with CMP populations (Figure 3D). This suggests that G9a inhibition is selectively affecting multipotent KLS populations (including HSCs and MPPs). Furthermore, the number of myeloid progenitors decreased in UNC0638 treated HSCs and MPPs (Figure 3D) suggesting that G9a inhibition both promotes self-renewal and inhibits differentiating divisions in these KLS cells. Based on their higher self-renewal potential, as expected, HSCs maintain higher KLS numbers compared to MPPs (Figure 3D-E). Based on these data, G9a selectively alters stem and progenitor populations, leading to retention and expansion of those cells capable of self-renewal.

In order to investigate whether G9a inhibition leads to increased self-renewal, we compared the cell cycle status of our *in vitro* cultured cells. HSCs and MPPs were plated and KLS or myeloid progenitor populations were analyzed by EdU

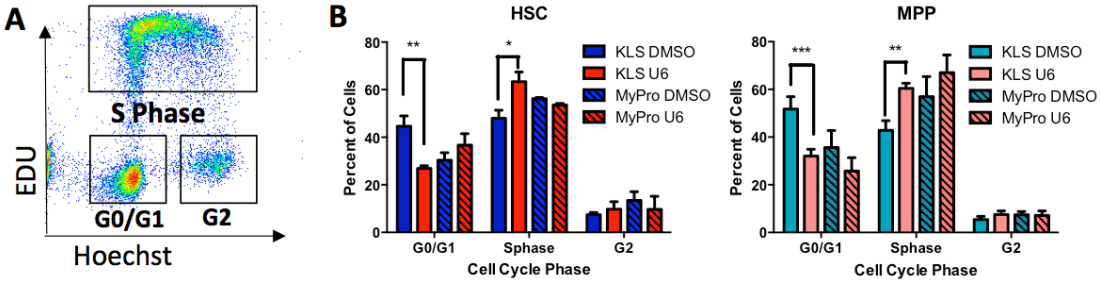

Figure 4. G9a inhibited HSCs and MPPs have a significantly higher percentage of KLS cells in S Phase. (A-B) Cell cycle analysis of Day 5 KLS or MyPro from cultured HSCs (KLS: n=3, MyPro: n=2) or cultured MPPs (KLS: n=6, MyPro: n=4) using EdU incorporation combined with Hoechst staining. P-values were determined using two-way ANOVA p*≤ 0.05, p**≤ 0.01, p***≤ 0.001, p****≤ 0.0001

incorporation after 5 days of culture. Both HSCs and MPPs treated with UNC0638 exhibited a highly significant increase in the number of cells in S phase at the expense of cells in G0/G1 phase (Figure 4A-B). Consistent with UNC0638's lack of effect on CMPs, we saw no significant difference in the cell cycle status between treated and control myeloid progenitors from HSCs or MPPs. Thus, G9a inhibition leads to increased numbers of replicating KLS cells, suggesting that UNC0638 leads to increased self-renewal divisions in these KLS populations.

Global levels of H3K9me2/3 do not change upon G9a inhibition

To investigate the mechanisms by which G9a leads to an increased KLS cell population, we first analyzed H3K9me2/3 levels in UNC0638 treated cells. Although G9a inhibition leads to differences in cell cycle and differentiation potential, we found that global levels of H3K9me2/3 were not altered upon G9a inhibition. UNC0638 treated cells trended towards lower levels of H3K9me3. However, there were no statistically significant differences in H3K9me2 or H3K9me3 levels in myeloid progenitor or KLS populations compared to DMSO treated myeloid progenitors with an n=2 (Figure 5A).

Overall levels of H3K9me2/3 remained unaltered, but perhaps G9a inhibition alters the nuclear distribution of H3K9me2/3 in UNC0638 treated KLS cells. Consistent with our western blot data, immunostaining detected no significant differences

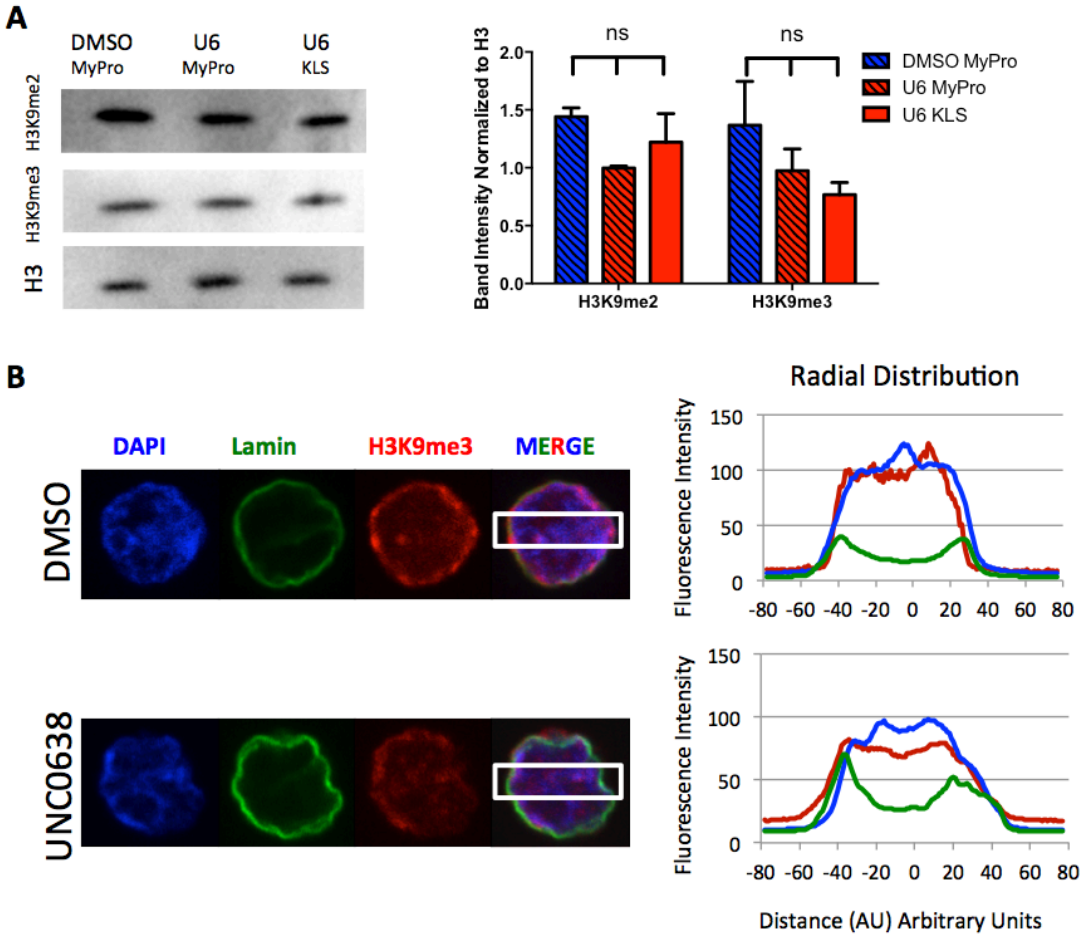

Figure 5. Global levels of H3K9me2/3 do not change upon G9a inhibition. Analysis of Day 5 culture of HSCs with UNC0638 or DMSO. (A) Western blot analysis of MyPro or KLS fraction normalized to H3 signal (n=2). DMSO treated KLS populations were not tested due to low cell numbers. (B) A representative image of DMSO & UNC0638 KLS collected on a Volocity spinning disk confocal system. Average radial distribution of 10 KLS cells, DAPI (blue), Lamin (green), & H3K9me3 (red) was quantified by fluorescence intensity across the middle section of the cell (white box).

in H3K9me3 nuclear distribution between UNC0638 and control populations (Figure 5B). We observed a few central foci of H3K9me3 which are consistent with previous publications (Gaspar-Maia et al., 2009). These data suggest that the effects of G9a inhibition may be caused by changes at a few specific genomic loci instead of a loss in overall H3K9me2/3 levels or a change in their nuclear spatial distributions. This is

supported by the observation that G9a-mediated H3K9 methylation leads to local changes in chromatin accessibility (Chen et al., 2014) rather than major global alterations.

G9a inhibition leads to changes in the expression of HSC associated genes

We next examined the global gene expression profile of UNC0638 treated cells to determine if changes in gene expression may explain our increase in KLS upon G9a inhibition. We performed RNA-seq on KLS populations from day 5 UNC0638 or DMSO *in vitro* treated HSCs. Among the up-regulated genes in the UNC0638 treated KLS cells, we found several genes directly associated with HSC function compared to MPP function, such as *Sox6, Itga2b, Gata1* and *Fgf3* (Gekas and Graf, 2013) (Figure 6A-B). We also identified significantly down regulated genes involved in the regulation of quiescence, such as *Egr1* (Min et al., 2008), *Ndn* (Asai et al., 2012), and migration, such as *Robo4* (Smith-Berdan et al., 2011) (Figure 6A). We verified our RNA-seq findings by RT-qPCR on these putative G9a target genes and, as expected, we found that UNC0638 treated cells had higher relative gene expression of these genes compared to the DMSO control (Figure 6C). Interestingly, in freshly isolated cells, several of these genes are significantly more highly expressed in HSCs compared to MPPs, suggesting that G9a inhibition prevents the silencing of genes necessary for the transition of HSCs into MPPs. Therefore, G9a inhibition leads to the expression of a more HSC-like gene expression profile compared to cells grown in the absence of UNC0638. These data support and help explain our earlier

observations that, upon G9a treatment, stem and progenitor populations are retained and have an increased ability to self-renew.

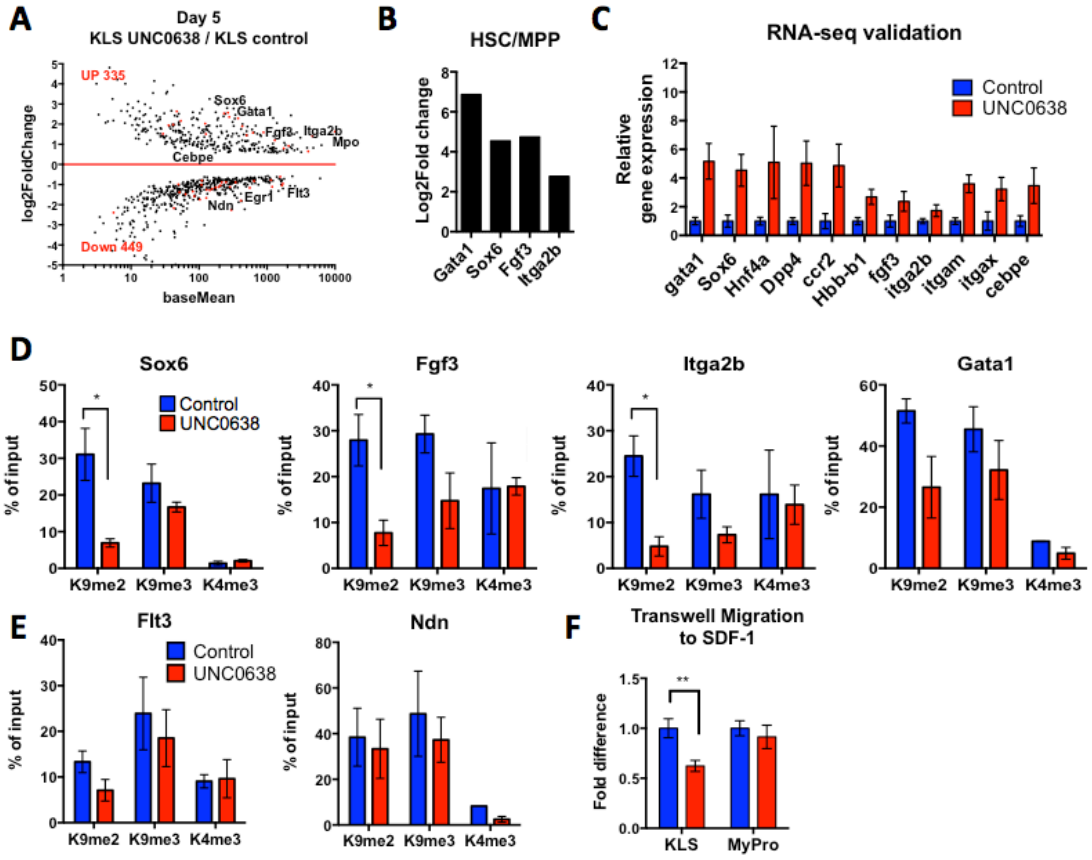

Figure 6. G9a inhibition leads to changes in the expression of HSC functional genes (A) Significantly up/ down regulated HSC-related genes identified by RNA-seq analysis (n=3) of cells treated with UNC0638 or DMSO (DESEQ padj<0.01, n=3). (B) Differential gene expression (log2fold change) of four genes identified as upregulated upon UNC0638 treatment in freshly isolated HSCs vs. MPPs. (C) qRT-PCR analysis of genes identified as upregulated in UNC0638 treated KLS cells by RNA-seq. (D) ChIP-qPCR for silencing mark H3K9me2/3 and active mark H3K4me3 on promoters of putative G9a targets identified as up-regulated (D) or down-regulated (E) from RNA-seq (n=3). (F) Transwell migration assay demonstrated an impaired capacity of UNC0638 KLS cells to migrate towards the chemokine SDF-1 n=3. Cells were sorted from day 5 cultures of HSCs incubated with or without UNC0638 and plated on methylcellulose. P-values were determined using t test p*≤ 0.05, p**≤ 0.01, p***≤ 0.001, p****≤ 0.0001

To explore whether changes in gene expression were a direct consequence of the loss of H3K9me2/3, we performed ChIP-qPCR for H3K9me2, H3K9me3, and the active

mark H3K4me3 on the promoters of these putative G9a targets. As expected, several up-regulated genes identified by RNA-seq had significantly lower amounts of H3K9me2 at their promoter (Figure 6D). These same genes trended towards lower amounts of H3K9me3, and unaltered levels of H3K4me3 compared to the control (Figure 6D). In contrast, genes identified as down regulated upon UNC0638 treatment had no significant changes in H3K9me2/3, suggesting that their down-regulation may be an indirect consequence of G9a inhibition (Figure 6E). Since gene expression profiling revealed misregulation of genes associated with hematopoietic migration in UNC0638 treated cells (data not shown), we performed transwell migration assays to determine whether UNC0638 treated cells displayed impaired migration towards the chemokine SDF1. We found a significant decrease in the migration efficiency of UNC0638 treated HSPCs, but not myeloid progenitors, compared to the DMSO control (Figure 6F). This suggests that HSPCs cells may have migration issues due to misregulation of important transcripts upon G9a inhibition. Our gene expression analysis suggests that at least some genes up-regulated upon G9a inhibition are directly silenced by G9a during differentiation. Therefore, we propose that during normal differentiation, G9a leads to silencing of specific regions, and that upon G9a inhibition, these genes are up-regulated, independent of H3K4me3.

UNC0638 treated cells maintain their functionality *in vivo*

Inhibition of G9a in HSCs leads to an accumulation of cells phenotypically described as stem and progenitor populations. Functional HSCs, by definition, are multipotent

and capable of long-term reconstitution in an irradiated host. In order to determine whether the KLS cells accumulating upon UNC0638 treatment are able to produce multiple lineages, 500 UBC-GFP KLS (UNC0638 or DMSO treated) were retro-orbitally transplanted into sub-lethally irradiated recipient mice (Figure 7A). Blood was tested for the presence of donor-derived red blood cells (RBCs), platelets, granulocytes/ macrophages (GM), B cells, and T cells over 14 weeks. UNC0638 cells reconstituted (>1% engraftment) all five lineages at similar ratios to the DMSO control cells (Figure 7B). However, UNC0638 treated cells trended towards overall

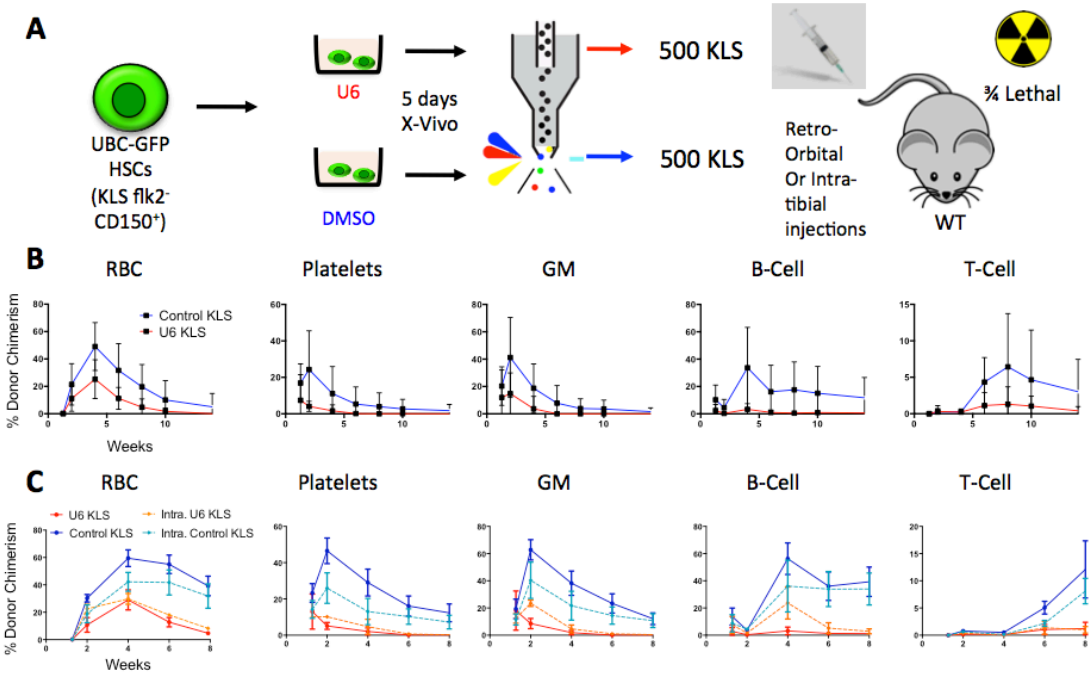

Figure 7. KLS populations from G9a Inhibition have multilineage reconstitution potential. Hematopoietic reconstitution of mice transplanted with *in vitro* UBC-GFP HSCs cultured with UNC0638 or DMSO. (A-C) 500 KLS from day 5 were injected (B) retro-orbitally (n=3, 4 mice per group) or (C) intra-tibially (directly into bone marrow, n=1, 4 mice per group) into sub-lethally irradiated wild-type (WT) recipients (also plotted with retro-orbital KLS data from same experiment). Red Blood Cells (RBC), Platelets, Granulocytes/ Macrophages (GM), B and T cells were detected from both conditions, with no significant difference in lineage distribution or percent donor chimerism. Intra-tibial injections show less difference in percent donor chimerism between UNC0638 and control populations compared to retro-orbital.

lower engraftment than their control counterparts. This was unexpected since both UNC0638 and control KLS cells were phenotypically HSPCs (Figure 3F for gating).

Since gene expression profiling revealed misregulation of genes associated with migration in UNC0638 treated cells, we hypothesized that the trend towards lower engraftment may be caused by migration defects. To test whether reduced migration efficiency could explain the failure of UNC0638-treated HSCs to engraft at higher levels than untreated cells, we injected 500 KLS (UNC0638 or DMSO treated) directly into the tibia bone of sub-lethally irradiated mice (Figure 7A). For the intra-tibial injections, UNC0638 treated KLS exhibited donor chimerism more similar to that of DMSO compared to the difference between populations in retro-orbital injections (Figure 7C). Although engraftment of UNC0638 treated compared to control was slightly improved upon intra-tibial injections, possible migration defects fail to account for all engraftment differences between UNC0638 and control transplants. These data suggest that, although G9a inhibition produces phenotypic KLS populations with multilineage potential, those cells are unable to match control levels of donor chimerism, even when bypassing full-body circulation.

We have established that G9a-inhibited KLS cells are able to read out in all lineages, so to further investigate potential functional differences in G9a treated HSCs, we assessed their ability to long-term engraft. Since *in vitro* cells have impaired ability to long-term engraft (Holyoake et al., 1997), HSCs were cultured for a shorter period

(24h) in the presence of UNC0638 or DMSO. Subsequently, 2,000 c-kit+ cells (KLS and myeloid progenitor fraction) were transplanted retro-orbitally into lethally irradiated recipients (Figure 8A). Cells grown in liquid culture for more than 24hr were unable to long-term engraft in control or UNC0638 conditions (data not shown). UNC0638 and control KLS populations under 24 hour conditions gave rise to all five

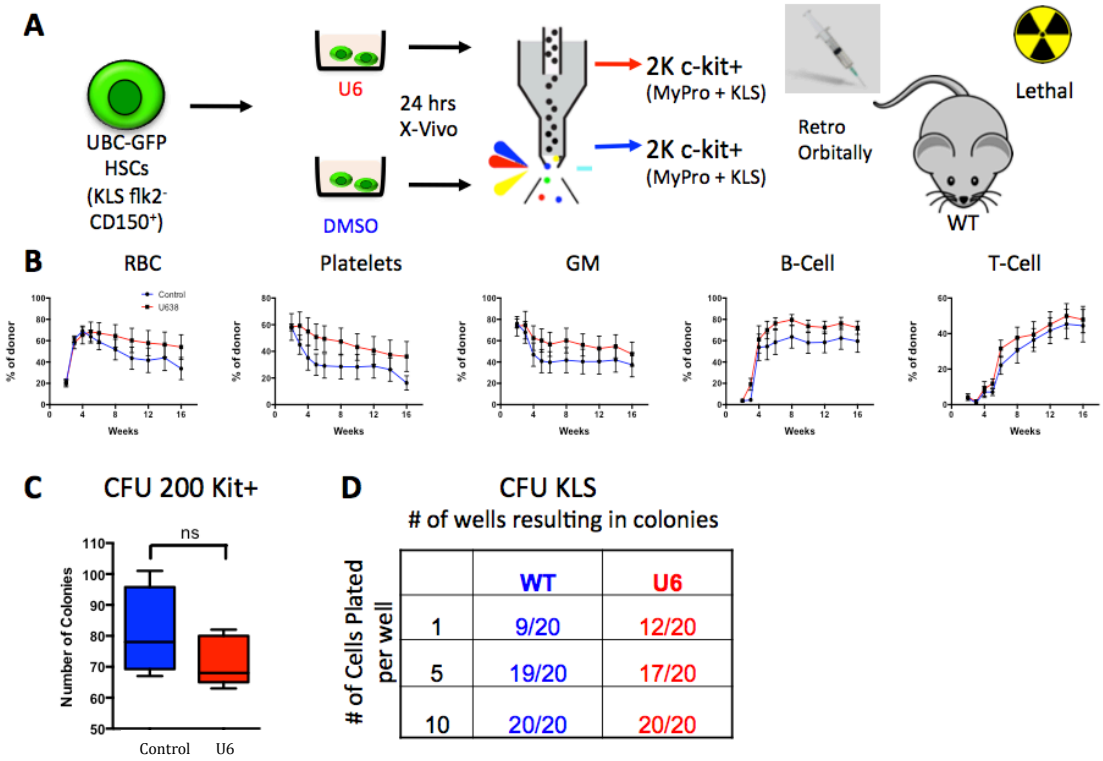

Figure 8. KLS populations from G9a Inhibition have long term, multilineage reconstitution potential and produce colonies similar to control. (A-B) Hematopoietic reconstitution of mice transplanted with *in vitro* UBC-GFP HSCs cultured in the absence or presence of UNC0638. 2K c-kit+ (MyPro + KLS) cells from 24h culture were transplanted retro-orbitally into lethally irradiated recipients (n=1, 8 mice per group). RBC, Platelets, GM, B and T cells were detected from both conditions, with no significant difference in lineage distribution or percent donor chimerism. UNC0638 treated cells were expected to exhibit a significantly higher reconstitution due to higher proportion of stem and progenitor KLS cells in the c-kit+ fraction. However, only a slight trend towards higher chimerism was observed. (C) Number of independent colonies formed from 200 control or UNC0638 c-kit+ cells (n=2). (D) Number of wells plated with 1, 5, or 10 control or UNC0638 KLS which gave rise to colonies (n=1). Data are means ± SEM, *$p < 0.05$, **$p < 0.01$, ***$p < 0.001$; ns, not significant. Statistical analysis by two-tailed t-test.

lineages and long-term engraftment past 12 weeks (Figure 8B). However, consistent with the results shown in Figure 7, UNC0638 populations (even after only 24 hour of treatment) read out lower given the proportion of KLS cells in c-kit^{+} fraction (UNC0638 c-kit^{+} fraction consists of more stem and progenitor cells [KLS] compared to DMSO c-kit^{+} fraction). Therefore, we would expect significantly more robust read out from the UNC0638 fraction than that shown in Figure 8B. Similar results were also produced in transplants with our original conditions on AFT layers (Figure 9A-B). Therefore, the KLS progeny of G9a treated cells give rise to all five hematopoietic lineages, are better able to match control reconstitution levels when directly injected into the bone marrow, and are able to long term engraft if transplanted after 24h in liquid culture or 5 days with AFT-layers.

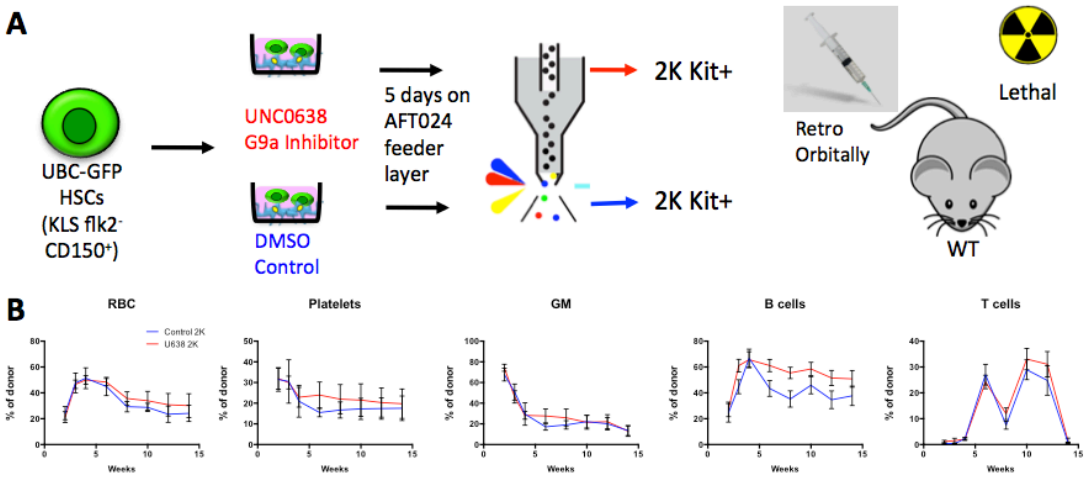

Figure 9. G9a Inhibition of HSCs on AFT024 feeder layers leads to multilineage reconstitution. (A-B) Hematopoietic reconstitution of mice transplanted with 2K *in vitro* c-Kit+ cells from HSCs cultured on AFT024 layers in the absence or presence of UNC0638. There was no significant difference in donor chimerism between conditions. (n=1, 7 mice per group).

Although they exhibit key characteristics of true HSCs and progenitors, G9a inhibited populations produce lower percentages of mature donor cells upon transplantation. One possibility is that only a fraction of c-kit+ cells from UNC0638 treatment are functional progenitors. To test this hypothesis, 200 c-kit+ cells from UNC0638 culture were plated in a colony forming unit (CFU) assay. Results demonstrated no significant differences in the number of colonies formed, suggesting that both UNC0638 and control have equivalent capability to form colonies (Figure 8C). To test the individual potential of UNC0638 treated cells, 1, 5, or 10 cells were sorted directly into wells containing methylcellulose (Figure 8D). Wells that produced colonies were counted. No significant difference in the ability to form colonies between UNC0638 treated and control was observed. Taken together, these results indicate that while G9a inhibited KLS populations are multipotent and capable of long-term reconstitution, in a transplant setting, these KLS cells have reduced ability to reconstitute irradiated hosts to the same degree as their control counterparts.

DISCUSSION

Previously, our lab established a model of HSC differentiation where heterochromatin formation increases during hematopoietic differentiation (Ugarte, Sousae et al., in submission). In order to address how heterochromatin formation affects HSC differentiation potential, we investigated the affect of inhibiting G9a, a writer of the heterochromatin associated histone mark H3K9me. H3K9me2 mediated by G9a has a critical role in general transcriptional silencing and regulation throughout

development (Jenuwein, 2006; Tachibana et al., 2002). More importantly, others have implicated the importance of G9a silencing of stem cell genes in other systems. G9a function, alongside DNA methylation, has been shown to regulate the timing of pluripotency gene silencing upon ESC differentiation (Yamamizu et al., 2012). Furthermore, iPSC reprogramming of Oct4/Klf4-transduced mouse embryonic fibroblasts was greatly enhanced by inhibition of G9a with a small molecule inhibitor (Shi, et al., 2008). Therefore, G9a inhibition may prolong stem cell capabilities by preventing the silencing of genes associated with differentiation. Here, we have shown that inhibition of G9a with the small molecule inhibitor UNC0638 in isolated HSCs leads to an increase in stem and progenitor progeny of HSCs *in vitro*.

Our ChIP data revealed that G9a inhibition leads to lower levels of H3K9me2/3 at key promoters associated with HSC identity, such as *Sox6* and *Gata1*. Global gene expression analysis confirmed that these same genes were significantly up regulated upon UNC0638 treatment. Together, these data suggest that silencing the production of specific transcripts through G9a is necessary for HSC differentiation, and inhibiting this process impairs the ability of stem and progenitor cells to differentiate. The importance of G9a during HSC differentiation has also been demonstrated in the human system where H3K9me2 chromatin territories are absent in primitive cells and are formed *de novo* during lineage commitment (Chen et al., 2012). Recently, H3K9me2 patterning has also been directly implicated in regulating chromatin

structure at promoters and other regions, wherein H3K9me2 specifically promoted "closed" chromatin conformations (Schones et al., 2014).

G9a inhibition leads to a KLS population capable of multilineage readout and long-term reconstitution, but surprisingly, these cells were unable to reach donor chimerism levels comparable to the control KLS cells. This observation indicates that G9a inhibition may affect other aspects of HSC function, such as migration. This possibility is supported by data from our intra-tibial injections, in which UNC0638 treated cells produced more similar donor chimerism to control transplants compared to the difference from retro-orbital, as well as global gene expression data indicating misregulation of genes involved in cell migration. Another possibility is that the lower engraftment is in part caused by higher rates of proliferation in G9a inhibited KLS (more in S phase compared to control). Evidence suggests that actively dividing cells do not engraft as well as more quiescent cells, such as true HSCs (Passegue et al., 2005; Hematopoietic Stem Cells, 2011). Transplanting G9a-inhibited, higher proliferating KLS could account for our less robust donor chimerism compared to the control.

Altogether our results offer a model where, upon G9a inhibition, failure to silence specific genomic regions leads to a delay in HSC differentiation. This reinforces global chromatin condensation as an essential regulator of stem cell lineage potential and differentiation during hematopoiesis. The next step would be to identify

mechanistically how G9a promotes differentiation of HSCs. By exploring putative G9a targets discovered in our gene expression data and the patterns of H3K9me2 during differentiation, we can better understand mechanisms of lineage potential and fate decision. Nevertheless, we have explored one piece of the puzzle and have shown that heterochromatin formation, in part through G9a-mediated histone methylation, is essential for the epigenetic regulation of HSC fate and function.

EXPERIMENTAL PROCEDURES

Mice All experiments were performed using 8–12 week old C57BL/6 wild type or C57BL/6-Tg(UBC-GFP) mice in accordance with UCSC guidelines. The mice were not euthanized for the sole purpose of this experiment and cells were acquired for other research as well.

Cell Isolation Hematopoietic cells were sorted from C57BL/6 wild type bone marrow from femurs & tibias as described (Forsberg et al., 2006). Stem and progenitor cell fractions were enriched using CD117-coupled magnetic beads (Miltenyi). The enriched fraction was stained with unconjugated lineage rat antibodies (CD3, CD4, CD5, CD8, B220, Gr1, Mac1, and Ter119) followed by goat-α-rat PE-Cy5 (Biolegend). Stem cells were isolated using c-kit-APC-Cy7, Sca1-PB, Slamf1-PECy7, CD34-FITC, FcγrII-PE and Flk2-biotin (all from Biolegend) followed by streptavidin-Qdot605 (Invitrogen) and were sorted using a FACS Aria II (BD Bioscience). HSPCs were defined as c-kit^{+}Lin^{-}Sca1^{+} (KLS) BM cells; HSCs as

Flk2^{-}, CD150^{+}, KLS cells; MPPs as Flk2^{+}, CD150^{-}, KLS cells; myeloid progenitors as c-kit^{+}Lin^{-}Sca1^{-} BM cells and mature hematopoietic cells as positive for cell surface expression of CD3 (T cells), CD4, CD5, CD8, B220 (B cells), Gr1, Mac1 ("GM" cells were positive for both Gr1 and Mac1), and/or Ter119 (Forsberg et al., 2006).

Electron microscopy Fixed cells were ultrathin sectioned on a Reichert Ultracut S ultramicrotome and counter-stained with 0.8% lead citrate. Grids were examined on a JEOL JEM-1230 transmission electron microscope and photographed with the Gatan Ultrascan 1000 digital camera at the Gladstone Institute EM facility, San Francisco, CA, followed by ImageJ analysis.

Soft X-ray Microscopy FACS sorted cells were mounted in thin-walled glass capillary tubes and rapidly cryo-immobilized prior to mounting in a cryogenic specimen rotation stage of the XM-2 Soft X-ray microscope (Le Gros et al., 2005). 3D tomograms were used for calculations and movies (Movies S1-S3).

Cell Culture FACS sorted HSCs (KLS Flk2-CD150+) were seeded at 100-500 cells into 96-well plates and grown in liquid culture: Xvivo15 media, 55uM Bme, Primocin (50 mg/ml), Tpo (5 ng/ml), SCF (25 ng/ml), Flt3L ligand (25 ng/ml), Il-3 (10 ng/ml), GM-SCF (10 ng/ml), or on ATF024 (ATCC- SCRC-1007) stromal cells: 1% PenStrep, 10% Fetal Bovine Serum in DMEM media (with glucose, L-glutamine, and sodium pyruvate), Tpo (5 ng/ml), SCF (25 ng/ml), Flt3L ligand (25 ng/ml), Il-3 (10

ng/ml) , GM-SCF (10 ng/ml). AFT024 layers were setup to 85% confluence the day before the co-culture with HSCs. Cells were cultured with 0.3uM UNC0638 (Sigma) or 0.3uM DMSO. When harvesting cells from AFT-Layers, cells were typsinized and the media and wash were collected with the sample. After harvesting, cells were analyzed for cell surface marker expression by flow cytometry. Hematopoietic cells were separated from the AFT024 cells based on CD45-APCCy7 (Biolegend) expression.

Western Blots: Cells were cultured with 0.3uM UNC0638 (Sigma) or 0.3μM DMSO in liquid culture conditions. After 5 days, cells were harvested and $1x10^4$ FACS sorted cells were lysed in RIPA buffer, and run in a 15% gradient SDS-page (BIO-RAD). Histone modifications were assessed with antibodies against H3K27me3 (07-449 Millipore), total H3 (06-755), H3K9me2 (Ab1220), and H3K9me3 (Ab8898).
For immunostaining, cells were sorted and placed into poly-lysine coated slides, fixed with 2% PFA, permeabilized with 0.1% triton-x in PBS, and stained with H3K9me3 (Ab8898), Lamin B (sc-6217) antibodies followed by an Alexa488-Donkey-α-goat and a Alexa594-goat-α-rabbit secondary antibody (Invitrogen) plus DAPI. Images were acquired using a PerkinElmer Velocity spinning disk confocal microscope. Image analysis was done using ImageJ software (Schneider et al., 2012)**.**

RNA-seq and ChIP-qPCR RNA-seq libraries from *in vitro* cultured cells were prepared using NEBNext® Ultra kit (New England Biolabs) following manufacturer

instructions. Libraries were sequenced using HiSeq2000 platform (Illumina) at the genomic sequencing laboratory, UC Berkeley, and analyzed with DESEQ software (Bioconductor.org). ChIP experiments were performed on *in vitro* cultured, FACS sorted, hematopoietic cells using SX-8G IPSTAR automated ChIP system (Diagenode) using 1ug of H3K4me3, H3K9me2, and H3K9me3 antibodies respectively. qPCR on ChIP DNA were performed with SensiMix SYBR® No-ROX kit (Bioline) and the ViiA7 system (Life Technologies).

Transplants & Read-out: Cells were cultured with 0.3μM UNC0638 (Sigma) or 0.3μM DMSO in liquid or AFT024 conditions. After 24 hours or 5 days, cells were harvested, sorted for KLS or MyPro, and transplanted into congenic, irradiated C57BL/6 mice. Cells transplanted into lethally irradiated hosts were accompanied by with $2x10^5$ Sca-1 depleted BM cells. Hematopoietic cells were separated from the AFT024 cells based on the GFP expression of hematopoietic cells as HSCs were derived from UBC-GFP mice). Equal amounts of c-kit+ or KLS cells were then transplanted into lethally irradiated C57BL/6 mice together with $2x10^5$ Sca-1 depleted BM cells. Consistent with previous reports (Moore et al., 1997; Nolta et al., 2002), use of AFT024 cells enhanced the ability of cultured HSCs to engraft long-term.

EdU Cell Cycle Analysis: Cell cycle analyses were performed using the Click iT EdU assay (Life Technologies) as per manufacturer's instructions.

***In vitro* Migration assays:** *In vitro* migration assays were performed in 5 mm pore size transwell inserts (Corning) towards SDF-1 (100 ng/ml, Peprotech) for 2 hours at 37°C, as described previously (Smith-Berdan et al., 2011).

CFU assays: HSCs were plated in liquid conditions with 3uM UNC0638 or 3uM DMSO for 5 days, then sorted to isolate ckit+ or KLS cells. Cells were mixed with methylcellulose medium (MethoCult 3434; Stem Cell Technologies) containing SCF (25ng/ml), Flt3 (25ng/ml), Il-6 (25ng/ml), TPO (25ng/ml), Il-3 (10ng/ml), EPO (2.5Units/ml), and GM-CSF (10ng/ml) and were dispensed into 30 mm dishes or 96-well plate using a sterile disposable 5 ml syringe with a 16 gauge blunt end needle. After 4 days incubation, the colonies were counted and scored.

REFERNCES

Akashi, Koichi, et al. "A clonogenic common myeloid progenitor that gives rise to all myeloid lineages." *Nature* 404.6774 (2000): 193-197.

Asai, T., Liu, Y., Di Giandomenico, S., Bae, N., Ndiaye-Lobry, D., Deblasio, A., Menendez, S., Antipin, Y., Reva, B., Wevrick, R., et al. (2012). Necdin, a p53 target gene, regulates the quiescence and response to genotoxic stress of hematopoietic stem/progenitor cells. Blood *120*, 1601–1612.

Boyer, Scott W., et al. "All hematopoietic cells develop from hematopoietic stem cells through Flk2/Flt3-positive progenitor cells." *Cell Stem Cell* 9.1 (2011): 64-73.

Buenrostro, Jason D., et al. "Transposition of native chromatin for fast and sensitive epigenomic profiling of open chromatin, DNA-binding proteins and nucleosome position." *Nature methods* (2013).

Chen, Xiaoji, et al. "G9a/GLP-dependent histone H3K9me2 patterning during human hematopoietic stem cell lineage commitment." *Genes & development* 26.22 (2012): 2499-2511.

Daigle, Scott R., et al. "Potent inhibition of DOT1L as treatment of MLL-fusion leukemia." *Blood* 122.6 (2013): 1017-1025.

Datta, Jharna, et al. "A new class of quinoline-based DNA hypomethylating agents reactivates tumor suppressor genes by blocking DNA methyltransferase 1 activity and inducing its degradation." *Cancer research* 69.10 (2009): 4277-4285.

Forsberg, E. Camilla, et al. "New Evidence Supporting Megakaryocyte-Erythrocyte Potential of Flk2/Flt3 Multipotent Hematopoietic Progenitors." *Cell* 126.2 (2006): 415-426.

Gaspar-Maia, Alexandre, et al. "Chd1 regulates open chromatin and pluripotency of embryonic stem cells." *Nature* 460.7257 (2009): 863-868.

Gekas, Christos, and Thomas Graf. "CD41 expression marks myeloid-biased adult hematopoietic stem cells and increases with age." *Blood* 121.22 (2013): 4463-4472.

Hasemann, Marie S., et al. "C/EBPα Is Required for Long-Term Self-Renewal and Lineage Priming of Hematopoietic Stem Cells and for the Maintenance of Epigenetic Configurations in Multipotent Progenitors." *PLoS genetics* 10.1 (2014): e1004079.

Hematopoietic Stem Cells. In *Stem Cell Information* [World Wide Web site]. Bethesda, MD: National Institutes of Health, U.S. Department of Health and Human Services, 2011 [cited Thursday, November 06, 2014] Available at http://stemcells.nih.gov/info/scireport/pages/chapter5.aspx

Holyoake, T. L., et al. "CD34 positive PBPC expanded ex vivo may not provide durable engraftment following myeloablative chemoradiotherapy regimens." *Bone marrow transplantation* 19.11 (1997): 1095-1101.

Jenuwein, Thomas. "The epigenetic magic of histone lysine methylation." *Febs Journal* 273.14 (2006): 3121-3135.

Krivtsov, Andrei V., et al. "H3K79 methylation profiles define murine and human MLL-AF4 leukemias." *Cancer cell* 14.5 (2008): 355-368.

Kubicek, Stefan, et al. "Reversal of H3K9me2 by a small-molecule inhibitor for the G9a histone methyltransferase." *Molecular cell* 25.3 (2007): 473-481.

Lara-Astiaso, David, et al. "Chromatin state dynamics during blood formation." *Science* 345.6199 (2014): 943-949.

Min, Irene M., et al. "The transcription factor EGR1 controls both the proliferation and localization of hematopoietic stem cells." *Cell Stem Cell* 2.4 (2008): 380-391.

Miranda, Tina Branscombe, et al. "DZNep is a global histone methylation inhibitor that reactivates developmental genes not silenced by DNA methylation." *Molecular cancer therapeutics* 8.6 (2009): 1579-1588.

Moore, Kateri A., et al. "Hematopoietic activity of a stromal cell transmembrane protein containing epidermal growth factor-like repeat motifs." *Proceedings of the National Academy of Sciences* 94.8 (1997): 4011-4016.

Ogawa M. Differentiation and proliferation of hematopoietic stem cells. Blood. 1993; 81(11): 2844–2853.

Passegué, Emmanuelle, et al. "Global analysis of proliferation and cell cycle gene expression in the regulation of hematopoietic stem and progenitor cell fates." *The Journal of experimental medicine* 202.11 (2005): 1599-1611.

Schones, Dustin E., et al. "G9a/GLP-dependent H3K9me2 patterning alters chromatin structure at CpG islands in hematopoietic progenitors." *Epigenetics & chromatin* 7.1 (2014): 23.

Seita, Jun, and Irving L. Weissman. "Hematopoietic Stem Cell: Self-renewal versus Differentiation." *Wiley Interdisciplinary Reviews: Systems Biology and Medicine* 2.6 (2010): 640-53. *PubMed*. Web. 14 Aug. 2014.

Shi, Yan, et al. "Induction of pluripotent stem cells from mouse embryonic fibroblasts by Oct4 and Klf4 with small-molecule compounds." *Cell stem cell* 3.5 (2008): 568-574.

Smith-Berdan, Stephanie, et al. "Robo4 cooperates with CXCR4 to specify hematopoietic stem cell localization to bone marrow niches." *Cell Stem Cell* 8.1 (2011): 72-83.

Stresemann, Carlo, and Frank Lyko. "Modes of action of the DNA methyltransferase inhibitors azacytidine and decitabine." *International journal of cancer* 123.1 (2008): 8-13.

Tachibana, Makoto, et al. "G9a histone methyltransferase plays a dominant role in euchromatic histone H3 lysine 9 methylation and is essential for early embryogenesis." *Genes & development* 16.14 (2002): 1779-1791.

Ugarte F, Sousae R, Cinquin B, Sanchez G, Inman M, Tsang H, Warr M, Passegue E, Larabell C, Forsberg CE. “Progressive chromatin condensation and H3K9 methylation regulate the differentiation of embryonic and hematopoietic stem cells.” Under Review

Vedadi, Masoud, et al. "A chemical probe selectively inhibits G9a and GLP methyltransferase activity in cells." *Nature chemical biology* 7.8 (2011): 566-574.

Wineman, John, et al. "Functional heterogeneity of the hematopoietic microenvironment: rare stromal elements maintain long-term repopulating stem cells." *Blood* 87.10 (1996): 4082-4090.

Yamamizu, Kohei, et al. "Protein kinase A determines timing of early differentiation through epigenetic regulation with G9a." *Cell stem cell* 10.6 (2012): 759-770.